Colloid Polym Sci 275:38–45 (1997)
© Steinkopff Verlag 1997

ORIGINAL CONTRIBUTION

Ts. Miteva
L. Minkova

Structure investigations of PE-g-LCP copolymers

Received: 3 April 1996
Accepted: 15 August 1996

Ts. Miteva · Dr. L. Minkova (✉)
Institute of Polymers
Bulgarian Academy of Sciences
1113 Sofia, Bulgaria

Abstract Transesterification products – copolymers of semiflexible liquid crystalline polymer SBH 112 grafted to functionalized low molecular mass polyethylene (PEox) obtained by melt polycondensation or reactive blending procedures have been investigated by wide-angle x-ray scattering (WAXS) and scanning electron microscopy (SEM).

The x-ray diffraction patterns of PE-g-LCP copolymers obtained via both procedures consist of reflections typical for the orthorhombic crystalline lattice of PE and the single reflection of the solid LCP. The lack of d_{hkl} variations with respect to those of neat PEox and SBH indicates the absence of interactions in the crystalline phase or that of cocrystallization phenomena between the components of the PE-g-SBH copolymers. The analysis of the crystallinity degree and normalized amorphous and crystalline contributions to the diffraction patterns of the products suggests that both copolymer components are partly miscible in the amorphous phase. The extent of miscibility depends on the copolymer structure, namely on the length of PE segments and SBH grafts. PE segments in PE-g-SBH copolymers obtained by the reactive blending are longer and exhibit a higher crystallizability than those obtained via melt polycondensation. SBH grafts of the copolymers obtained by the reactive blending are also longer than those in the products obtained via melt polycondensation.

The morphology of the samples has been interpreted as determined by the different structure of the copolymers obtained by both procedures.

Key words PE-g-LCP copolymers – WAXS investigations – crystallinity – morphology

Introduction

Much attention is being paid to blends of commercial thermoplastics with liquid crystalline polymers (LCPs) to develop high performance composites [1, 2]. The blends' morphology and the resulting physical properties are strongly influenced by the interaction between the matrix polymer and the LCP. For the particular case of polyolefin/LCP blends the affinity of the matrix polyolefin with thermotropic aromatic copolyesters and copolyesteramides is too low to grant adequate compatibility. This fact has normally led to blends with no improvement of the mechanical properties [3–5]. As for the blends of polyethylene (PE) and LCPs, the few studies performed so far [6–11] confirm that even using semiflexible LCPs the poor compatibility of the components remains and leads to low interfacial adhesion and non-uniform dispersion of the LCP phase, i.e., it prevents the attainment of good blend morphologies. Better results have been achieved [11] for blends of linear low density PE (LLDPE) and semiflexible LCP SBH 112 [12]. These blends have a more uniform distribution of the LCP phase in the PE matrix and consequently slightly improved mechanical properties. These results have been attributed to a bit better compatibility between LLDPE and this semiflexible LCP.

It is believed copolymers possessing segments with chemical structure similar to those of the polymers blended play the role of compatibilizing agents which promotes interfacial adhesion and renders a finer and more uniform distribution of the dispersed LCP phase. Better dispersion and adhesion result in improved mechanical properties of the compatibilized blends [13, 14]. The procedure of reactive blending involves *in situ* reaction of functional components forming block or graft copolymer at the interface between the phases. Another possibility for compatibilization is to add a preformed block or graft copolymer to the binary blend as a third component through preblending with the matrix polymer [13, 14] or with the LCP. There are different synthetic routes for preparing these block and graft copolymers as prospective compatibilizers.

In previous papers [15, 16] two main procedures for obtaining a PE-g-LCP copolymer and the preliminary attempts for their usage as compatibilizers in PE/LCP blends have been described. The first procedure involves polycondensation of the LCP monomers in the presence of functionalized PE (PEox). The second is the reactive blending of the PEox with preformed LCP. The copolymers formed were proved and investigated by IR spectroscopy, solid state ^{13}C NMR, DSC, thermogravimetry and SEM. It was shown that during the first procedure a fairly quantitative reaction of the carboxyl groups of the functionalized PE takes place, while only a part of PEox carboxyl groups undergo the transesterification during the second procedure [15, 16]. Better understanding of the crystalline structure and morphology of the PE-g-LCP copolymers is necessary to confirm their potential to act as compatibilizers. In cases of different polymer blends with crystallizable components the x-ray diffraction method is reliable to find the degree of order of the LCP phase in the blend and its influence on the crystallinity of the matrix [17, 18] as well as to examine the crystallizability of the copolymer segments [19]. The aim of the present work is to study the crystalline structure and morphology of PE-g-LCP copolymers obtained by polycondensation or reactive blending [15, 16] with respect to their application as PE/LCP blends compatibilizers.

Experimental

The functionalized PE (PEox) sample was supplied by Aldrich. This oxidized PE has an acid number of 28 mg KOH/g and a molar mass of ca. 10 000, which correspond to approximately 5 carboxylic groups per mol. The LCP was a laboratory sample of SBH 112 (Sebacic acid-S; 4,4′-dihydroxybiphenyl-B; 4-hydroxybenzoic acid-H) kindly provided by Eniricerche SpA, Milan. This LCP has a crystalline to nematic phase transition temperature of 230 °C.

The transesterification products – copolymers of SBH grafted on PEox were obtained by two main procedures [15, 16]. According to the first procedure the SBH synthesis is carried out in the presence of PEox which carboxyl groups are capable of entering the polycondensation reaction [15]. The product obtained (COP) consists chiefly of PE-g-SBH with a wide range of component content and of negligible amount of unreacted PEox. The second procedure consists of the catalyzed transesterification reaction between PEox and preformed SBH carried out in a Brabender mixer for different mixing time (15, 60, 120 min). This procedure (reactive blending) leads to products COP15, COP60 and COP120 containing appreciable amounts of unreacted PEox together with the formed copolymer PE-g-SBH [16]. For comparison a physical blend of PEox and SBH in the same 50/50 w/w ratio was prepared in the Brabender mixer without catalyst for mixing time 6 min. All the above products are successively fractionated with boiling toluene and xylene – good solvents for PEox and PE-g-SBH copolymers with low SBH content. The composition of the soluble fractions and the residues, determined thermogravimetrically [15, 16] is summarized in Table 1.

WAXS investigations of the neat components PEox and SBH, of the transesterification products (as crystallized from melt) and of their soluble and insoluble fractions (as crystallized from the corresponding $\sim 1\%$ solutions after the fractionation) were carried out at room temperature in a powder URD diffractometer, using Ni-filtered CuK$_\alpha$ radiation (1.54 Å). The diffraction scans were collected over a period of ca. 130 min between 2θ values of 10 and 50° in reflectance mode using a step of 0.1°. The computer program FIT [20] was used for decomposition of the powder diffraction patterns. After an automatic background correction, the peaks were detected by the maxima of the fourth experimental profile derivatives. Pseudo-Voight analytical function was used for the profiles fitting. The obtained parameters of the individual peaks were used for further calculations: PE d_{hkl} spacings were calculated from the Bragg equation using the peaks corresponding to reflections along the (110) and (200) planes; the half-widths were used to determine the crystallite size from the Scherer formula; the peaks areas were used to calculate the PE crystallinity degree in the samples as a ratio of the areas of PE crystalline peaks (110) and (200) (Ac) and the sum of Ac and total amorphous area of the sample (Aa) [18]. The fitted profile of COP pattern is shown for example on Fig. 1.

SEM observations of the samples crystallized from solution were made on a Jeol T550 apparatus.

Table 1 Composition of the investigated samples

Sample	Symbol	Composition PE/SBH w/w
Mechanical blend	MIX	50/50
– soluble toluene	NCM	100/0
– insoluble	RXM	0/100
Reactive blend at 15 min	COP15	50/50
– soluble toluene	NCC15	89/11
– insoluble	RXC15	0/100
Reactive blend at 60 min	COP60	50/50
– soluble toluene	NCC60	100/0
– insoluble	RXC60	90/10
Reactive blend at 120 min	COP120	50/50
– soluble toluene	NCC120	100/0
– soluble xylene	SXC120	73/27
– insoluble	RXC120	27/73
Copolymer	COP	50/50
– soluble toluene	NCC	80/20
– soluble xylene	SXC	65/35
– insoluble	RXC	27/75

Fig. 1 An example separation of crystalline and amorphous regions on the COP diffractogram

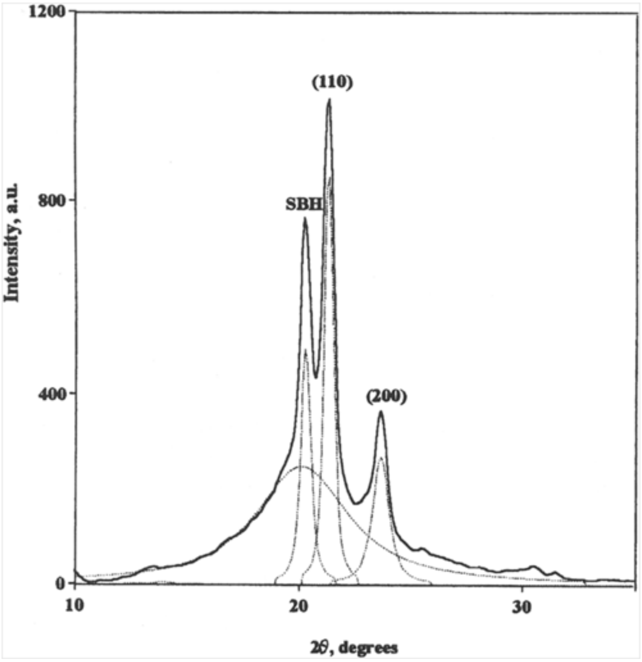

Results and discussion

The x-ray diffraction patterns of melt crystallized samples of neat components, MIX, COP and COP120 are reported in Fig. 2. The d_{hkl} spacings calculated from the peaks corresponding to the main reflections of the components are presented in Table 2. For the neat PEox sample the most intense diffraction peaks are observed at $2\theta = 21.3°$, $23.6°$, $36.0°$ corresponding to reflections along (110), (200), (020) crystallographic planes of the orthorhombic crystalline lattice of polyethylene, respectively [19]. Reflections of monoclinic or triclinic phase of polyethylene are not seen on the x-ray diffractogram of PEox. The calculated dimensions of the PEox unit cell correspond to an orthorhombic lattice of a branched polyethylene. As shown previously [12], the x-ray pattern of the neat SBH presents a single reflection at $2\theta = 20.3°$ corresponding to a spacing of ca. 4.4 Å [12]. This reflection of the solid LCP is due to the lateral packing of parallel oriented macromolecules having cylindrical symmetry and longitudinal disorder [12].

Fig. 2 X-ray diffractograms of the neat components and of MIX, COP and COP120

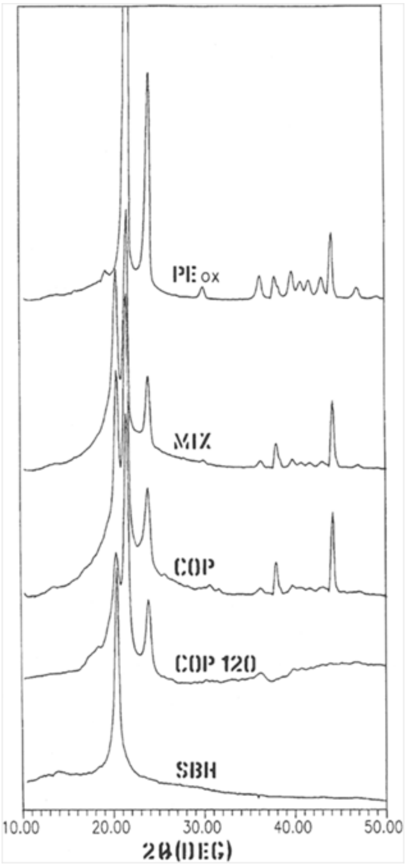

Table 2 Values of the d_{hkl} spacings of the samples and average PE crystallites sizes

Sample	d_{SBH} (Å)	d_{110} (Å)	d_{200} (Å)	L_{PE} (Å)
PEox	–	4.17	3.76	339
MIX	4.38	4.15	3.74	330
COP15	4.38	4.16	3.75	285
COP60	4.37	4.15	3.74	278
COP120	4.36	4.14	3.74	295
COP	4.37	4.15	3.74	290
NCM	–	4.15	3.74	340
NCC15	4.35	4.13	3.73	307
NCC60	–	4.14	3.75	304
NCC120	–	4.15	3.74	331
SXC120	4.31	4.13	3.73	282
NCC	–	4.14	3.74	295
SXC	4.32	4.13	3.73	279
RXM	4.37	–	–	
RXC15	4.35	–	3.77	–
RXC60	4.37	4.16	3.75	126
RXC120	4.34	4.12	3.72	168
RXC	4.30	4.08	3.68	119
SBH	4.37	–	–	–

The diffraction patterns of the mechanical blend MIX and of the transesterification products COP, COP15, COP60 and COP120 consist of the reflections of both components (Fig. 2 and Table 2). That means both components PE and SBH form separate crystalline phases not only in the mechanical blend but also in the transesterification products where they are bonded chemically. It has to be mentioned that in all MIX, COP15, COP60 and COP120 the ratio of both components is of 50/50 w/w. That is why it is worth studying the diffraction patterns of the soluble and insoluble fractions where the ratios of both components are different (Table 1). The x-ray diffraction patterns of COP120 fractions are shown in Fig. 3 and those of the insoluble fractions of COP, COP15, COP60 and COP120 in Fig. 4. The d_{hkl} spacings calculated from the peaks corresponding to the main reflections of PE and SBH observed on the x-ray patterns are listed in Table 2.

The diffractograms of NCM, NCC60 and NCC120 show no evidence of the SBH peak at $2\theta = 20.3°$ as could be expected of their compositions (Table 1). Surprisingly, the toluene soluble fraction of COP (NCC) also shows no evidence of such a peak, although a content of 20 wt% SBH grafts is determined thermogravimetrically for the PE-g-SBH copolymer in this fraction (Table 1). That means SBH grafts in the latter copolymer can not form a separate crystalline phase. It can be assumed that, being too short, SBH grafts are included only in the amorphous phase of the copolymer.

The diffractograms of the fractions NCC15, SXC120 and SXC, consisting of PE-g-SBH copolymers with SBH content of 11 ÷ 35 wt%, show evidence of the SBH peak at $2\theta = 20.3°$. These results show that SBH grafts of PE-g-SBH copolymers in these three fractions form individual crystalline phase. It is worth noting that the relative intensity of this peak of NCC15 pattern is negligible in comparison with those of SXC120 and SXC, inspite of the not so large difference in their SBH content. Evidently, the relative intensity of the SBH peak does not exactly correspond to the SBH content of the copolymers. The latter fact could mean an including of a part of the SBH grafts in the amorphous phase of the copolymers.

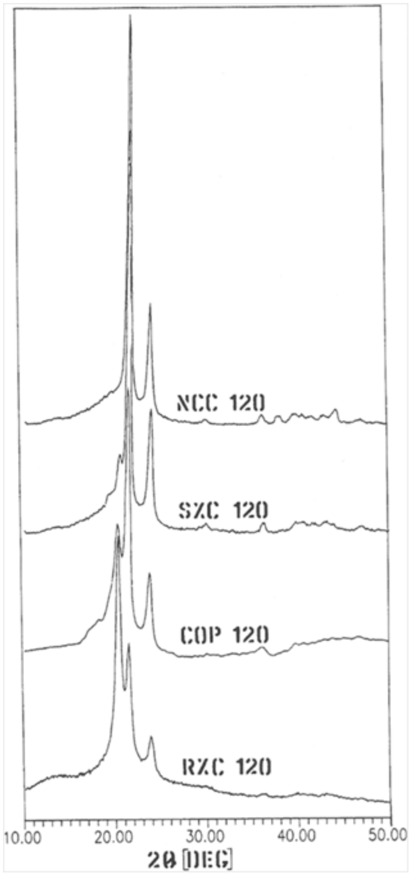

Fig. 3 X-ray diffractograms of COP120 and its soluble (NCC120 and SXC120) and insoluble (RXC120) fractions

Concerning PE-g-SBH copolymers, in which SBH component predominates (namely in the residues RXC, RXC15, RXC60 and RXC120), their x-ray patterns consist of reflections of both PE and SBH crystalline phases. It is interesting to note that the relative intensities of PE reflections are higher in RXC120 than in RXC pattern, inspite of the almost equal PE content of the two PE-g-SBH copolymers. PE reflections in RXC15 diffractogram are slightly observable, thus confirming that the residue RXC15 consists mainly of pure SBH.

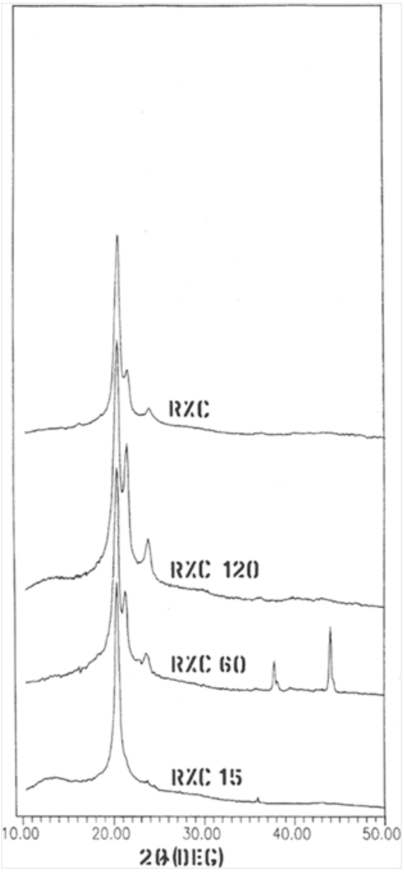

Fig. 4 X-ray diffractograms of the insoluble fractions of COP and of the reactive blends

Table 3 Comparison of x-ray peak areas of the samples

Sample	$\frac{Ac}{Ac+Aa}$	$\frac{Aa^s}{Aa^{pe} \cdot w^{pe}}$	$\frac{Ac^s}{Ac^{pe} \cdot w^{pe}}$	$\frac{Ac^s}{Ac^{pe}} : \frac{Aa^s}{Aa^{pe}}$
PEox	0.65	1.0	1.00	1.0
MIX	0.33	3.0	0.75	4.0
COP15	0.32	3.3	0.85	3.9
COP60	0.32	3.1	0.78	4.0
COP120	0.33	3.1	0.81	3.8
COP	0.28	4.6	0.94	4.9
NCM	0.61	1.00	1.00	1.0
NCC15	0.58	1.60	1.55	1.0
NCC60	0.58	1.80	1.60	1.1
NCC120	0.61	1.40	1.40	1.0
SXC120	0.46	2.10	1.10	1.9
NCC	0.50	2.30	1.30	1.8
SXC	0.41	2.45	1.17	2.1
RXC15	0.02	–	–	–
RXC60	0.11	–	–	–
RXC120	0.18	–	–	–
RXC	0.11	–	–	–

Using the peaks corresponding to PE reflections along (110) and (200) planes the PE d_{110} and d_{200} lattice spacings were calculated from the Bragg equation (Table 2). No significant variations of these values for PE component of the copolymers in a wide composition range can be seen. Analogously, the single reflection *d*-spacing corresponding to SBH has no significant variations for all of the samples in which scans the SBH peak is detectable. Such results evidence no interactions in the crystalline phase or of cocrystallization phenomena between the two components of the PE-g-SBH copolymers.

In order to gain insight into the nature of the copolymer crystalline behavior, we have tried to determine PE degree of crystallinity as follows: PE degree of crystallinity has been assumed as a ratio of the PE main peaks areas Ac and the sum of these areas and amorphous areas of the diffractogram Aa, namely (Ac/(Ac + Aa)), as it is done in [18]. The amorphous area on each diffractogram was drawn in one and the same angle interval using one and the same curve profile (as was done for neat PEox) (Fig. 1) in order to minimize the errors normally appearing for such complicated systems as copolymers. Such determined PE degree of crystallinity of the samples is presented in Table 3.

It should be noted that for the mechanical blend MIX and reactive blends COP15, COP60, COP120, the values of Ac/(Ac + Aa) are almost twice lower than the corresponding value of pure PEox, as could be expected according to the sample composition (Table 1). On the other hand, PE degree of crystallinity of COP is lower than those of MIX, COP15, COP60 and COP120. PE degree of crystallinity of NCM and NCC120 almost coincides with that of the neat PEox, thus confirming the sample composition (Table 1). PE degree of crystallinity of NCC15, NCC, SXC120 and SXC decreases with increasing the amount of SBH grafts (Table 3). Concerning PE degree of crystallinity of the insoluble fractions it is seen that Ac/(Ac + Aa) values increase in the range RXC15, RXC60, RXC120, i.e. with increasing the mixing time when preparing the reactive blends. Surprisingly, PE degree of crystallinity of RXC (insoluble fraction of COP) is lower than that of RXC120, although RXC and RXC120 have almost the same composition. In Fig. 5 the dependence of Ac/(Ac + Aa) on the mixing time for reactive blends COP15, COP60 and COP120 and their soluble and insoluble fractions is presented; the corresponding values for COP and its fractions NCC and RXC are given as single black points.

These results show that the Ac/(Ac + Aa) values do not exactly correspond to the sample composition (i.e. to the content of PE and SBH components as determined thermogravimetrically). The dependence PE crystallinity degree versus compositions of the samples was determined by relating the amorphous (Aa^s) and crystalline areas (Ac^s)

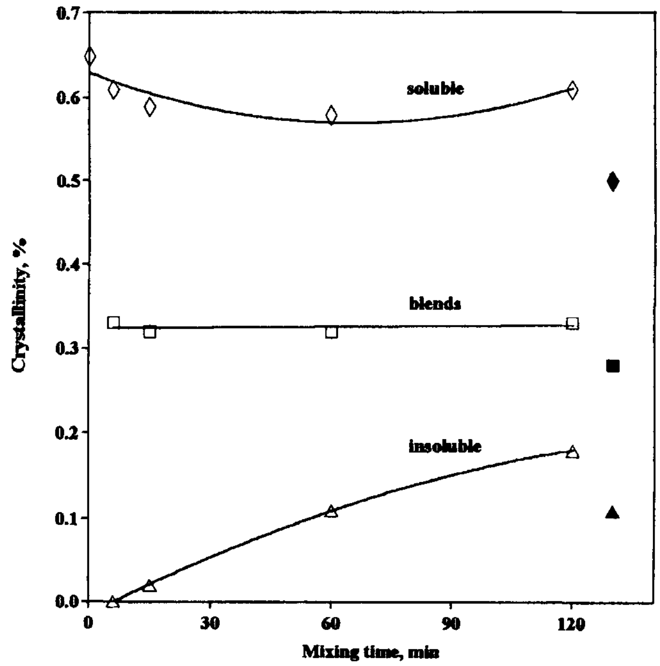

Fig. 5 Dependencies of the PE crystallinity on the mixing time for the reactive blends and their fractions (corresponding values for COP are given as single black points)

of the diffraction pattern of a given sample to the corresponding areas on the diffractogram of the neat PEox (Aa^{PE} and Ac^{PE}) and normalizing them to the weight fraction of PE (W^{PE}) in the sample, i.e., calculating relative amorphous $Aa^{s}/(Aa^{PE}\cdot W^{PE})$ and crystalline areas $Ac^{s}/(Ac^{PE}\cdot W^{PE})$. It should be pointed out that for the samples crystallized from melt (COP, COP15, COP60 and COP120) pattern areas were related to the corresponding areas of the pattern of PEox also crystallized from melt. For the samples crystallized from solution (soluble and insoluble fractions) the areas were related to the corresponding areas of the pattern of NCM. It could be seen from the data obtained (Table 3), that for MIX, COP15, COP60 and COP120 the relative crystalline areas $Ac^{s}/(Ac^{PE}\cdot W^{PE})$ decrease slightly while the relative amorphous areas $Aa^{s}/(Aa^{PE}\cdot W^{PE})$ increase strongly in comparison with those of neat PEox. Following these changes, the determined degree of crystallinity of these samples is almost twice lower than those of neat PEox. Contrary, the crystalline area of COP is practically unaffected while the relative amorphous area increases markedly, thus leading to a lower value of PE degree of crystallinity (Table 3). This increase in the relative amorphous area of COP could be explained by the fact that a part of the SBH grafts are included in the amorphous phase of the system. Concerning the soluble fractions, the following dependencies have been established: the relative amorphous and crystalline areas of NCC15, NCC60 and NCC120, consisting of almost pure PE, increase similarly, thus leading to the same PE degree of crystallinity as of neat PEox, while a strong increase of the relative amorphous areas is observed for NCC, SXC and SXC120, containing 20 ÷ 35 wt% SBH grafts (Table 1). Taking into account that the relative crystalline areas on the diffractograms of these sample change slightly, it is also supposed that a part of the SBH grafts of the copolymers are included in the amorphous phase of the systems. Evidently, all SBH grafts in PE-g-SBH copolymer in NCC (SBH content of ca. 20 wt%) enter the amorphous phase. The ratios of the relative crystalline $Ac^{s}/(Ac^{PE}\cdot W^{PE})$ and amorphous areas $Aa^{s}/(Aa^{PE}\cdot W^{PE})$ for a given sample were also calculated (Table 3). As expected, the calculated values for NCM, NCC15, NCC60 and NCC120 are close to 1. For NCC, SXC and SXC120 they are close to 2. Such results indicate an increase of the amorphous areas which is twice higher than that of the relative crystalline areas. Analogously, the ratio for MIX, COP15, COP60 and COP120 is of ca. 4 while for COP it is of ca. 5.

The analysis of the x-ray patterns and the calculated parameters allows to assume that: PE-g-SBH copolymers with SBH contents equal or lower than 50 wt%, the PE segments crystallize in an individual crystalline phase; the shorter SBH grafts are totally included in the amorphous phases of the systems until the longer ones form individual crystalline phases. Therefore, PE and SBH components can be mixed partially in the amorphous state. Evidently, the structure (i.e. the length of PE crystallizable segments and of SBH grafts) of the soluble COP copolymers and that of the soluble copolymers of the reactive blends is different, i.e. SBH grafts of the souble COP copolymers are shorter than those of COP15, COP60 and COP120.

Concerning the insoluble fractions, where SBH content is higher than 50 wt% (RXC, RXC15, RXC60 and RXC120), PE degree of crystallinity has been calculated with a lower precision due to the relatively lower intensity of the PE crystalline peaks on the diffractograms. Inspite of this, PE degree of crystallinity of RXC120 is evidently higher than that of RXC although the two copolymers have an equal content of SBH grafts. That means PE crystallizable segments in the two residues differ in length, i.e. the latter should to be shorter in RXC PE-g-SBH copolymer.

The PE crystallite sizes, determined according to Scherrer formula after separation of the apparative reflection width [20], are collected in Table 2. The average PE crystallite size is of ca. 304 ÷ 340 Å for the samples where the PE component is not chemically bonded to SBH. For the PE-g-SBH copolymers with SBH content lower that 50 wt% this size is reduced to 278 ÷ 296 Å. These results are interpreted by disturbance of the crystallization of PE segments bonded with relatively short SBH grafts. For the PE-g-SBH copolymers with SBH content higher than 50 wt% PE crystallite sizes are strongly reduced due to the worsened crystallizability of PE segments bonded to relatively long SBH grafts. It is worth noting that PE crystallite sizes in RXC are smaller than those in RXC120. This proves that PE crystallizable segments of PE-g-SBH copolymers in RXC are shorter than those in RXC120.

Summarizing all x-ray investigations, we can state that: both type of copolymers consist of long PE backbones and SBH grafts, but the copolymers obtained by polycondensation (COP) are with shorter PE segments and SBH grafts than those obtained by reactive blending.

It was also very interesting to study the morphology of PE-g-SBH with different SBH content and structure. On Fig. 6 the SEM micrographs of three types of samples crystallized from ca. ~1 wt% solutions are presented: of NCC120, containing almost pure PEox (Fig. 6a), of SXC120, containing PE-g-SBH copolymer with 27 wt% SBH grafts long enough to form individual crystalline phase (Fig. 6b) and of NCC, containing copolymer with 20 wt% SBH grafts included in the amorphous phase of the system (Fig. 6c). On the SEM micrograph of NCC120 (Fig. 6a) well defined detached multilyer hedrites can be observed, as expected for PE crystallized from 1 wt% solution. On the SXC120 micrograph these detached hedrite structures cannot be observed – the morphology is of polygonal particles (1–5 μm in diameter) forming compact aggregates. The morphology of NCC (Fig. 6c) is homogeneous and it does not resemble either the morphology of NCC120 or that of SXC120. The morphology of this PE-g-SBH copolymer with 20 wt% SBH grafts could be described as of "thickened lamellar like structures". Evidently, the differences in the observed morphologies are due to the different content and length of the SBH grafts in different copolymers.

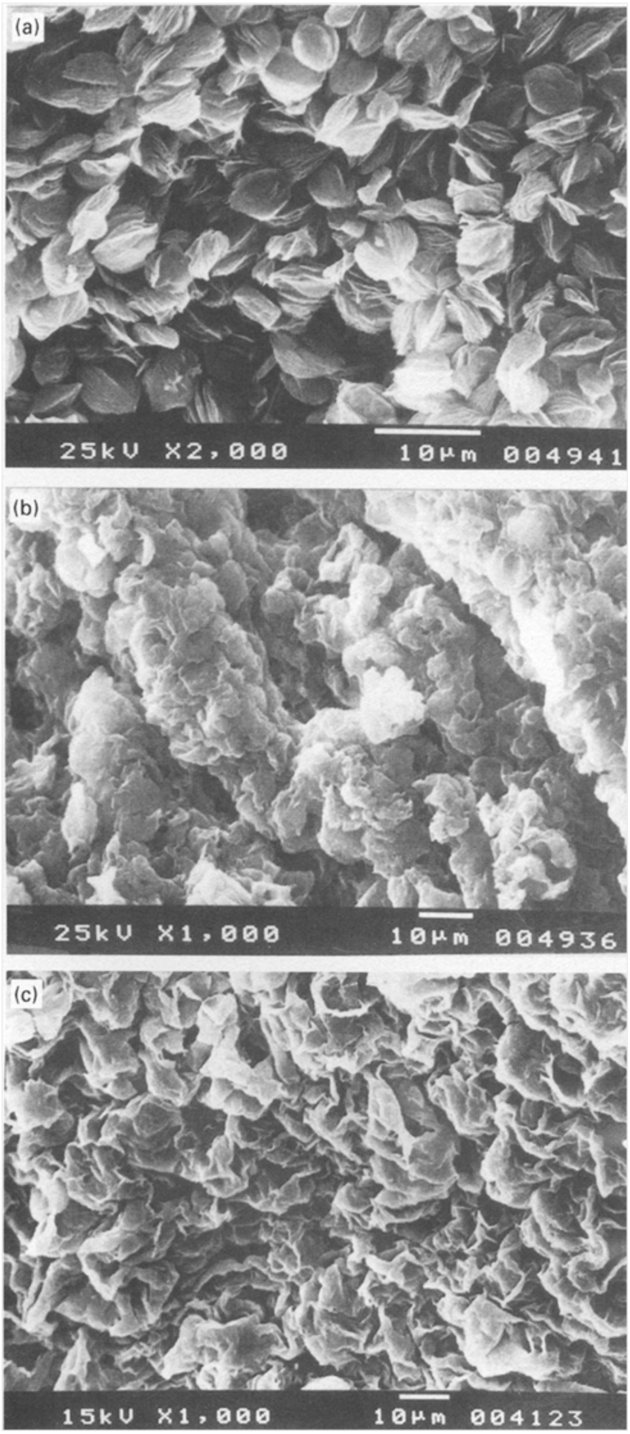

Fig. 6 SEM micrographs of the toluene and xylene soluble fractions of COP120–NCC120 **A** and SXC120 **B** resp., and of toluene soluble fraction of COP–NCC **C**

Conclusions

From the analysis of the x-ray diffraction patterns the crystalline structure of the copolymers obtained by the two synthetic procedures has been determined. It was revealed that no interactions occur in the crystalline phase between the copolymer components for the two copolymers, prepared by polycondensation and reactive blending. The copolymer components are partly miscible in the amorphous phase, depending on the length of SBH grafts.

It could be inferred that by the first procedure involving SBH synthesis in the presence of PEox copolymers with shorter PE crystallizable segments and SBH grafts have been prepared, whereas the second procedure consisting of reactive blending of PEox with preformed SBH leads to copolymers with longer PE crystallizable segments and SBH grafts. The latter are long enough to form crystalline structures similar to those of the neat polymers. That is why it could be assumed that these copolymers prepared by reactive blending would be more effective as compatibilizers for PE/SBH blends than those prepared by polycondensation.

Acknowledgments This work was carried out within a Copernicus Programme (Contract n.CIPA-CT94-0118) funded by the Commission of the European Communities. The authors thank Prof. P.L. Magagnini from the University of Pisa, Italy for the useful discussion.

References

1. Dutta D, Fruitwala H, Kohli A, Weiss RA (1990) Polym Eng Sci 30:1005
2. La Mantia FP (ed) (1993) Thermotropic Liquid Crystalline Polymer Blends. Technomic, Lancaster
3. Done D, Sukhadia AM, Datta A, Baird DG (1990) SPE Tech Pap 48:1857
4. Datta A, Sukhadia AM, Desouza JP, Baird DG (1991) SPE Tech Pap 49:913
5. Yongcheng Y, La Mantia FP, Valenza A, Citta V, Pedretti U, Roggero A (1991) Eur Pol J 27:723
6. Hsu TC, Lichkus AM, Harrison IR (1993) Polym Eng Sci 33:860
7. Hsu TC, Harrison IR (1993) SPE Antec'93, p 1183
8. Lichkus AM, Harrison IR (1992) SPE Antec'92, p 2257
9. Pedretti U, Roggero A, La Mantia FP, Magagnini PL (1993) SPE Antec'93, p 1706
10. Fernandes EG, Giolito I, Chiellini E (1994) Thermochim Acta 235:67
11. La Mantia FP, Geraci C, Vinci M, Pedretti U, Roggero A, Minkova LI, Magagnini PL (1995) J Appl Pol Sci 58:911
12. Pedretti U, Roggero A, Citta V, Montani E, La Mantia FP, Magagnini PL (ed) (1993) Processing and Properties of Liquid Crystalline Polymers and LCP Based Blends. Chem Tec Publishing, Canada
13. Datta A, Chen HH, Baird DG (1993) Polymer 34:759
14. Datta A, Baird DG (1995) Polymer 36:505
15. Magagnini PL, Paci M, Minkova LI, Miteva Ts, Sek D, Grobelny J, Kaczmarczyk B (1996) J Appl Polym Sci 60:1665
16. Minkova LI, Miteva Ts, Sek D, Kaczmarczyk B, Magagnini PL, Paci M, La Mantia FP, Scaffaro R, J Appl Polym Sci, in press
17. Ko CU, Wilkes GL, Wong CP (1989) J Appl Polym Sci 37:3063
18. Pracella M, Dainelli D, Galli GC, Chiellini E (1986) Makromol Chem 187:2387
19. Wunderlich B (1973) In: Macromolecular Physics. Academic Press, New York and London, vol. 1
20. Petkov V, Bacaltchev N (1990) J Appl Cryst 23:138